Korean Journal of Remote Sensing, Vol.19, No.1, 2003, pp.53~59

Inverse Brightness Temperature Estimation for Microwave Scanning Radiometer

Hyuk Park*, Vladimir Katkovnik*, Gum-Sil Kang*, Sung-Hyun Kim*, Jun-Ho Choi*, Se-Hwan Choi*, Jing-Shan Jiang, Yong-Hoon Kim***

Department of Mechatronics, Kwangju Institute of Science and Technology*
Center for Space Science and Applied Research, Chinese Academic of Science**

Abstract : The passive microwave remote sensing has progressed considerably in recent years. Important earth surface parameters are detected and monitored by airborne and space born radiometers. However the spatial resolution of real aperture measurements is constrained by the antenna aperture size available on orbiting platforms and on the ground. The inverse problem technique is researched in order to improve the spatial resolution of microwave scanning radiometer. We solve a two-dimensional (surface) temperature-imaging problem with a major intention to develop high-resolution methods. In this paper, the scenario for estimation of both radiometer point spread function (PSF) and target configuration is explained. The PSF of the radiometer is assumed to be unknown and estimated from the observations. The configuration and brightness temperature of targets are also estimated. To do this, we deal with the parametric modeling of observation scenario. The performance of developed algorithms is illustrated on two-dimensional experimental data obtained by the water vapor radiometer.

Key Words : Microwave Radiometer, Brightness Temperature Estimation, Inverse Problem.

1. Introduction

Radiometry or microwave remote sensing is a technique that provides information about a target based on its microwave radiation. We call the amount of microwave radiation energy the brightness temperature. From brightness temperature measurements, some target image can be reconstructed as different objects have different brightness temperatures.

An imaging radiometer maps the brightness temperature distribution over a field of view (FOV). A real aperture radiometer does it by scanning the FOV either mechanically across. Let us assume that the FOV is flat and $T(x, y)$ be an actual brightness temperature distribution given as a function of the Cartesian coordinates x and y. It is assumed that the radiometer moves with respect to the FOV in a plane parallel to the FOV. Assume also that the antenna beam of radiometer is perpendicular to the FOV. This measurement scenario is illustrated in Fig. 1.

Received 3 January 2003; Accepted 25 January 2003.

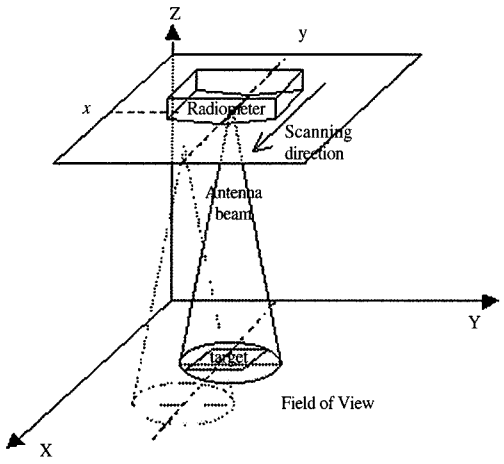

Fig. 1. Measurement scenario.

The measurement equation is presented in the form of

$$V(x, y) = \iint g(u, v) \cdot T(x+u, y+v)\, dudv \qquad (1)$$

the convolution (Ruf *et al.*, 1988),

where $g(u, v)$ is a cross-section of the antenna beam pattern with the FOV and u, v are coordinates defining a shift of the center of the beam footprint with respect to the current coordinates (x, y) of the FOV. Actually the formula (1) serves as an input-output observation model and $g(u, v)$ includes effects of electronic circuits, properties of a thermal emission and propagation media, etc. In the more general terms $g(u, v)$ is called a point spread function (PSF) or weight-function (kernel) of the radiometer, which summarizes all its properties forming the output measurement signal as a function of the true brightness temperature distribution $T(x, y)$.

In the equation (1), the resolution of the image is determined by the antenna beamwidth of the radiometer. A single-antenna radiometer usually has a comparably wide beam and as a result quite a poor resolution. To improve the resolution, we treat the measurements as a set of joint data

$$U_N = \{V(x_k, y_k), k = 1, 2, \cdots, N\} \qquad (2)$$

which are processed simultaneously. In this way the imaging of a single-antenna radiometer can be improved significantly. Here we refer to the so-called inverse problem methods, which are used, for deconvolution of the equation (1) in order to yield an estimate of the brightness temperature function $T(x, y)$ from observations U_N.

It is known that the finding $T(x, y)$ from the equation (1) belongs to the class of the so-called ill-conditioned problems (Madisetti *et al.*, 1997). Consequently, the conventional Fourier and inverse Fourier transform algorithms have a number of drawbacks.

Let us assume that the PSF as well as the targets (shapes, sizes, locations ad temperatures) are defined within unknown parameters. Then the brightness temperature estimation is equivalent to estimation of the mentioned parameters of the observation scenario. In this parametric case, imaging problem can be reformulated as fitting (matching) observation data by the parametric model.

This matched filtering approach was used in (Katkovnik *et al.*, 2001) for one-dimensional experimental data processing to get two dimensional brightness temperature distribution. It was shown that the problem can be solved for simple scenarios characterized by a small number of unknown parameters to be estimated. In this paper, this technique is extended to two-dimensional data interpretation.

2. Proposed Algorithm

We consider the following matched filtering specification of the problem (Katkovnik *et al.*, 2001). It is assumed that the approximate model of the observations (1) has a form of

$$\hat{V}(x, y) = \iint g(u, v, C_1) \cdot T(x+u, y+v, C_2)\, dudv \qquad (3)$$

where C_1 and C_2 are vector-parameters of the PSF and the temperature field respectively.

The quality-of-fit criteria is given as

$$Q(C_1, C_2) = \sum_{(x,y)\in U} F(e(x, y))$$
$$e(x, y) = V(x, y) - \hat{V}(x, y) \quad (4)$$

where $V(x, y)$ and $\hat{V}(x, y)$ denote respectively the experimental data and their approximation by the model (3) and U is a set of experimental data. We use two types of the loss function: $F = e^2$ and $F = |e|$.

As a starting point we apply a **two-step algorithm** (Katkovnik *et al.*, 2001):

Step 1: A calibration of the radiometer, i.e. an identification of the PSF $g(u, v, C_1)$. The vector parameter C_1 is estimated at this step. It is assumed that the experimental data U^0 are obtained for known brightness temperature target ("standard" temperature target) are used :

$$\min_{C_1} Q_0(C_1, C_2^0) \Rightarrow \hat{C}_1 \Rightarrow g(u, v, \hat{C}_1)$$
$$Q_0(C_1, C_2^0) = \sum_{(x,y)\in U^0} F(e(x, y)) \quad (5)$$

where $C_2 = C_2^0$ provides the accurate actual brightness temperature field as a function $T(x, y, C_2^0)$.

Step 2: A reconstruction of the brightness temperature field of an unknown target. The parameter C_2 of the unknown brightness temperature is estimated at this step:

$$\min_{C_2} Q_1(\hat{C}_1, C_2) \Rightarrow \hat{C}_2 \Rightarrow T(u, v, \hat{C}_2)$$
$$Q_1(C_1, C_2) = \sum_{(x,y)\in U^1} F(e(x, y)) \quad (6)$$

where another set of the experimental data U^1 is used corresponding to experiments with targets which brightness temperature, size and position are unknown.

However, the standard target cannot be available in many practical circumstances. Then, the following **one-step blind calibration** algorithm can be used. This algorithm is formalized follows:

$$\min_{C_1, C_2} Q_0(C_1, C_2) \Rightarrow (\hat{C}_1, \hat{C}_2)$$
$$\Rightarrow T(x, y, \hat{C}_2), g(u, v, \hat{C}_1)$$
$$Q(C_1, C_2) = \sum_{(x,y)\in U^2} F(e(x, y)) \quad (7)$$

In the one-step blind calibration algorithm we find the parameters of the PSF $g(u, v, C_1)$ as well as the temperature field $T(x, y, C_2)$ of interest as a solution of one optimization problem (7) simultaneously and it does not require the "standard" target measurements.

Sometimes, the matched filtering does not allow identify all unknown parameters. In particular, the measurements $V(x, y)$ in (1) is a product of the gain of the PSF and the brightness temperature. Thus, we are not able to separate this gain and the brightness temperature. In this case, only relative brightness temperature can be found.

The criteria function $Q(C_1, C_2)$ can happened to be rough, multimode without strong minimums. It might mean that the experimental data allow a number of different interpretations. Then, the problems (5) and (7) have a many different solutions. It ca be an objective fact affecting a reality of our experimental scenario allowing multiple solution.

However, sometimes it just shows that the used criteria functions are not relevant to the scenario. Then, it is necessary to try another ones in attempt to find the criteria demonstrating more definite behavior as well as giving as unique solution. We wish to describe the mathematical difficulties of the procedures (5) and (7) regularizing multi variable minimization of antenna functions which are not convex.

3. Experimental Results

The experimental scenario is depicted in Fig. 2. The background of the temperature field is formed from an absorbing material and various plate targets are fixed on

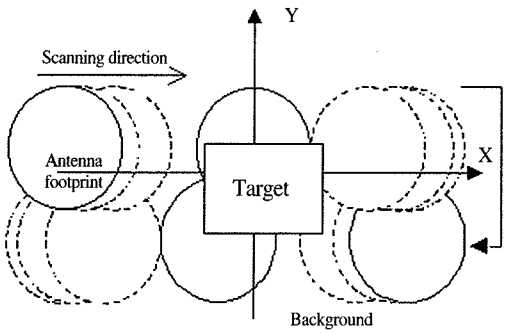

Fig. 2. Experiment scenario.

this background. The background and the radiometer were installed on ground. The distance between the radiometer and the target is 350 cm enough to satisfy far-field condition. This experiment is performed with water vapor radiometer with 6° half-power beamwidth and the equivalent footprint is 30.5 cm. Two-dimensional scanning along the X and Y-axis is performed. The scanning spacings are 6 cm for Y direction and 10 cm for X direction. The average temperature is 26°C when the experiment was performed

Unknown variables are as follows:

(a) The two-dimensional PSF of the radiometer;

(b) Location, orientation and sizes of the targets;

(c) Brightness temperature of the targets.

Thus, the basic intention is to reconstruct the two-dimensional temperature field of the targets and the radiometer PSF.

The results presented in this paper are obtained for three scenarios: "single" target, "two" separate targets and "complex targets" combined from four single targets. Each targets is assumed to have invariant brightness temperature distribution on their surface. The experiments are produced for two frequencies Ω_1 = 36 GHz and Ω_2 = 23 GHz. The blind calibration one-step

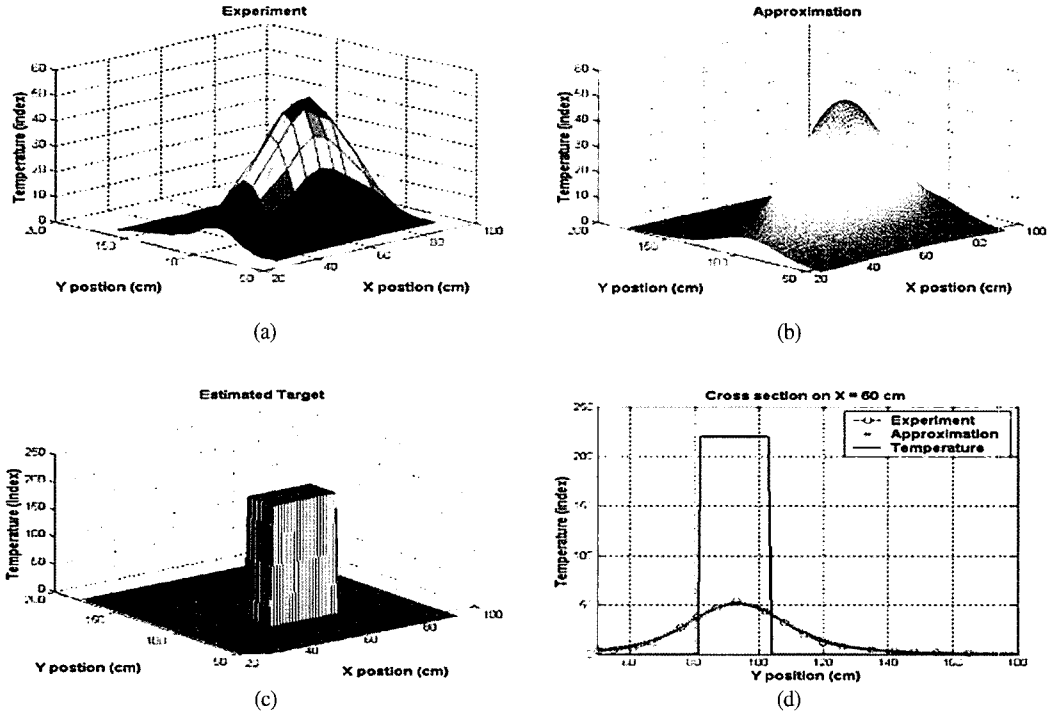

Fig. 3. Experiment and signal processing results of Test 1 for 31 GHz. (a) Experiment data. (b) Approximation. (c) Estimated Target. (d) Cross section view.

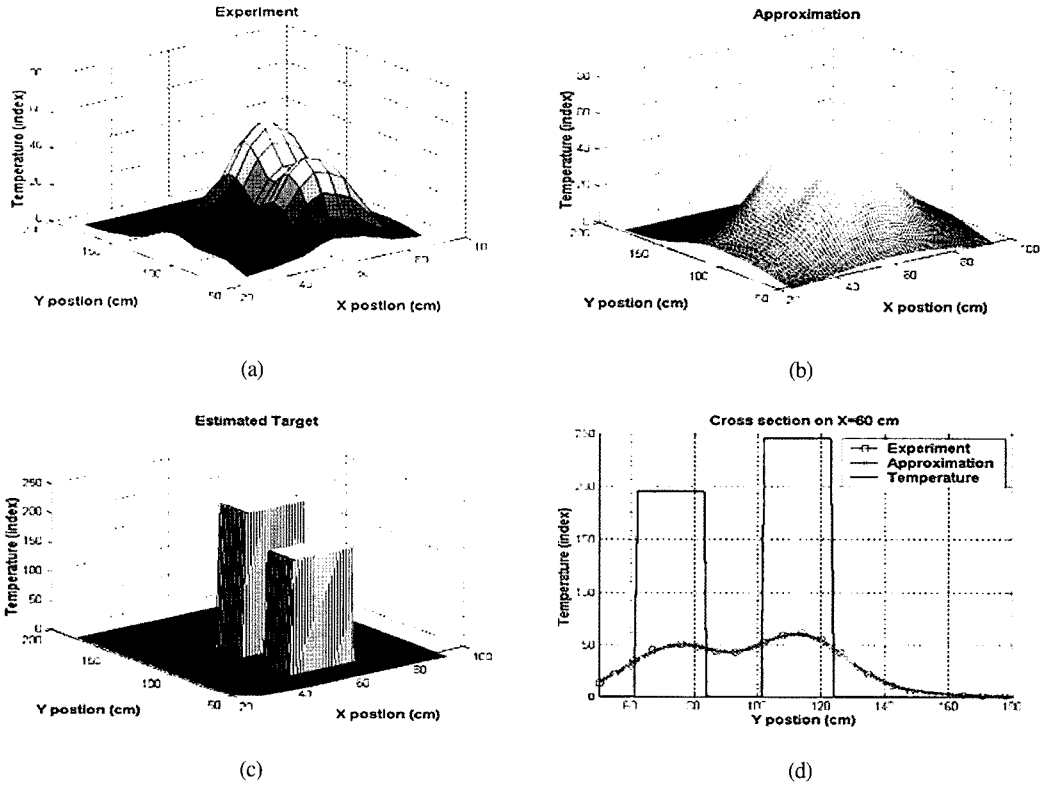

Fig. 4. Experiment and signal processing results of Test 2 for 31 GHz. (a) Experiment data. (b) Approximation. (c) Estimated Target. (d) Cross section view.

algorithm is used in order to calibrate the PSF. The calibrated PSF is supplied for data processing as it is defined in step 2 of the two-step algorithm. As candidates for the weight-function we considered a number of non-negative functions symmetric with the respect to the origin with the best fit of the experimental data found for

$$g(x,y) = K \cdot \exp\left[-\left\{(x/\alpha)^2 + (y/\alpha)^2\right\}^{\beta}\right] \tag{8}$$

$$K = 1/\sum_{m \in U} g(x_m, v_m)$$

where α and β are parameters. Therefore parameter C_1 of PSF in (5) is $C_1 = (\alpha, \beta)$. The beam shape of the radiometer is characterized by this parameter. The equation (8) has similar shape of Gaussian function and we can control the beamwidth and sharpness of the $g(x, y)$ by changing the $C_1 = (\alpha, \beta)$.

Test 1. "Single" target (20cm × 20cm, square shape, metal). The experimental observations as well as signal processing results are shown in Fig. 3. Fig. 3 (a) is the two-dimensional measurement of the radiometer. Fig. 3 (b) is the best fitting model by using equation (3) and one-step blind calibration. The parameter of PSF is C_1 = (16, 0.58).This parameter is obtained "Step 1 equation (5). Fig. 3 (c) shows the found target configuration and Fig. 3 (d) is the cross section of the found target, experimental data and fitting. One significant point is that presented temperature is not a real brightness temperature but a pre-processed temperature index. In other words, subtracting observed brightness temperatures from their maximum value produces the represented temperature indexes. It is done for the

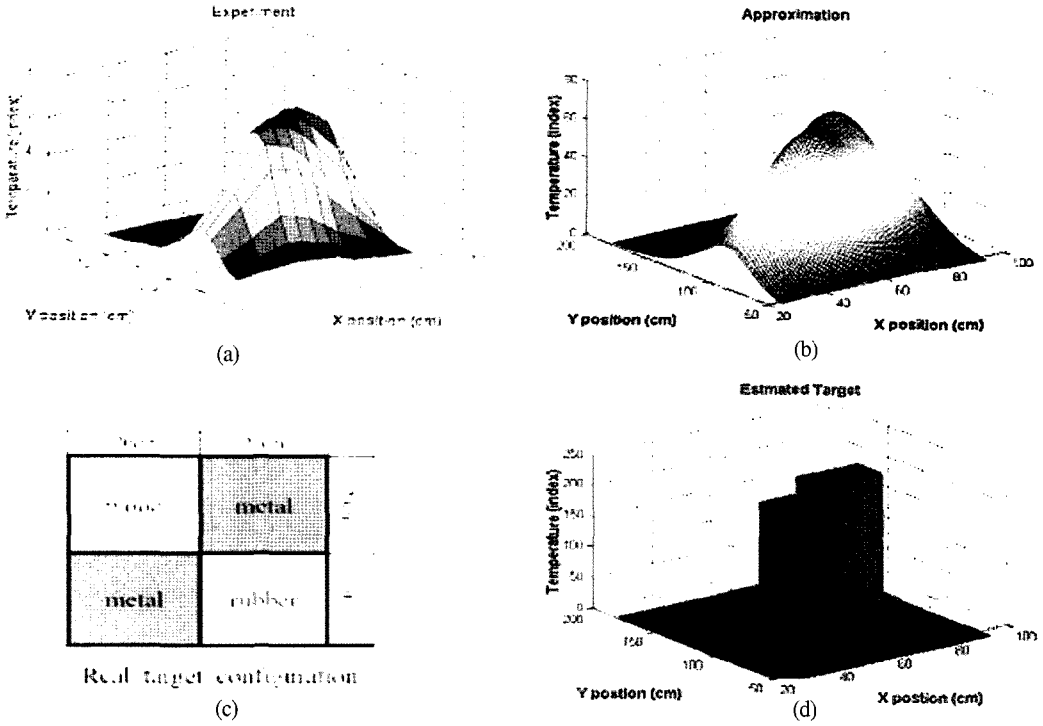

Fig. 5. Experiment and signal processing results of Test 3 for 31 GHz. (a) Experiment data. (b) Approximation. (c) Actual target configuration. (d) Estimated target configuration.

convenience of data processing and presentation. As a result, the 302K which is the actual maximum brightness temperature observed in Test 1 becomes the index value equal to 0 and minimum temperature 252K becomes the index value equal to 50.

In Test 1, the parameter of temperature field, C_2 of (3), defines a location, shape, size and brightness temperature of a "single" target. The found target brightness temperature is 220 indexes and the size is 21cm×21cm. The size estimate is quite accurate. The temperature estimate is also considered to be accurate because brightness temperature of metal is known to be around 225 indexes for outdoor measurements. For 23 GHz measurements, the algorithm also gives quite accurate results. Therefore, the results of Test 1 show that the proposed algorithm is feasible for two-dimensional data estimation and interpretation.

Test 2. "Two" separate targets (two 20cm×20cm, square shape, metal, with 20 cm spacing between the targets). In Test 2, the more complex configuration of targets is tested. The experimental observations as well as signal processing results are shown in Fig. 4. Test 2 is not a blind calibration but a reconstruction of the unknown targets with the PSF found in Test 1, $\alpha = 16$, $\beta = 0.58$.

The measurement, best fitting, found target configuration and cross section plot are shown in Fig. 4 (a), (b), (c) and (d), respectively. The brightness temperatures of targets are estimated as 195 and 245 indexes. The estimates of target sizes are both 20cm× 21cm. The estimate of the distance between them is 19 cm. Thus, restored target configurations are very close to real configuration and the estimated temperature indexes are also close to the value of Test 1.

Test 3. "Complex targets" combined from four single targets. Finally, we test somewhat complicated

configuration of target. The actual target configuration, experiment and signal processing results are illustrated in Fig. 5. The signal processing of Test 3 is more complex and difficult than it is for Test 1 and Test 2. The measurement surface is more complex to fit. In order to fit closely, we use many parameter components in C_2 of equation (6). Even though the complexity of the signal processing, the estimated configurations of targets are very close to actual target configurations. The estimated brightness temperatures of the two metal plates are 240 indexes. The estimated temperature of rubber and wood plate are 50 and 30 indexes, respectively. Generally rubber and wood have lower temperature by about 200 indexes than metal. Therefore, the good estimation accuracy is achieved and it means that the proposed algorithm is applicable in this scenario.

4. Conclusions

The matched filtering method is proposed in order to obtain high-resolution 2-D brightness temperature estimation and identification of the PSF of microwave radiometer. The experimental data processing shows good accuracy of estimation and reasonable interpretation of the brightness temperature distribution. The developed algorithms are applicable for the parametric scenarios of the problem. A further study is planed for using minimax criteria of the data fitting instead of the average criteria in (4) and for development more efficient calculation procedures for multivariable optimization. Furthermore, the experiments in various environments such as target material, shape and orientation will be performed.

Acknowledgements

This work was supported by the Advanced Environmental Monitoring Research Center in K-JIST and the international collaboration program with Center for Space Science and Applied Research (CSSAR), Chinese Academic of Science funded by MOST.

References

Tijhuis, A. G., K. Belkebir, A. C. S. Litman, and B. P. de Hon, 2001. Theoretical and Computational Aspects of 2-D Inverse Profiling, *IEEE Trans. on Geoscience and Remote Sensing*, 39(6): 1316-1330.

Ruf, C. S., C. T. Swift, A.B. Tanner, and D. M. Le Vine, 1988. Interferometric Synthetic Aperture Microwave Radiometry for the Remote Sensing, *IEEE Trans. on Geoscience and Remote Sensing*, 26(5): 597-611.

Madisetti, V. K. and D. B. Williams, 1997. *The Digital Signal Processing Handbook Section VII: Inverse Problems and Signal Reconstruction*, CRC Press and IEEE Press.

Katkovnik, V. and H. Park, 2001. Inverse Adaptive 2D Brightness Temperature Estimation for Microwave Radiometer, *Proc. of International Symposium on Remote Sensing*, pp. 341-345.